Slope streaks on Mars: Correlations with surface properties and the potential role of water

Norbert Schorghofer,[1,2] Oded Aharonson,[1,2] and Samar Khatiwala[1,3]

Received 16 July 2002; revised 5 September 2002; accepted 6 September 2002; published 12 December 2002.

[1] The Mars Orbiter Camera on board the Mars Global Surveyor spacecraft has returned images of numerous dark streaks that are the result of down-slope mass movement occurring under present-day martian climatic conditions. We systematically analyze over 23,000 high-resolution images and demonstrate that slope streaks form exclusively in regions of low thermal inertia (confirming earlier results), steep slopes, and, remarkably, only where peak temperatures exceed 275 K. The northernmost streaks, which form in the coldest environment, form preferentially on warmer south-facing slopes. Repeat images of sites with slope streaks show changes only if the time interval between the two images includes the warm season. Surprisingly (in light of the theoretically short residence time of H_2O close to the surface), the data support the possibility that small amounts of water are transiently present in low-latitude near-surface regions of Mars and undergo phase transitions at times of high insolation, triggering the observed mass movements. *INDEX TERMS:* 6225 Planetology: Solar System Objects: Mars; 1824 Hydrology: Geomorphology (1625); 5470 Planetology: Solid Surface Planets: Surface materials and properties. **Citation:** Schorghofer, N., O. Aharonson, and S. Khatiwala, Slope streaks on Mars: Correlations with surface properties and the potential role of water, *Geophys. Res. Lett.*, *29*(23), 2126, doi:10.1029/2002GL015889, 2002.

1. Introduction

[2] Preserved in the Martian geologic record are landforms reflecting an ancient wetter and perhaps warmer period. Geomorphic features such as dendritic valley networks and outflow channels have been interpreted as evidence of extensive fluvial activity in the early history of Mars [*Carr*, 1996; *Baker*, 2001]. Subsequent to this early period, the martian surface has been mostly very dry [*Baker*, 2001] and present atmospheric conditions are such that water or ice on the surface is generally unstable in the long term [*Ingersoll*, 1970; *Farmer and Doms*, 1979]. The discovery of small gullies in images obtained by the Mars Orbiter Camera (MOC) on board the Mars Global Surveyor (MGS) spacecraft has reopened the possibility of near-surface liquid water in the more recent past [*Malin and Edgett*, 2000], although there is no direct evidence for their active formation on present-day Mars. In contrast, slope streaks presently forming on the surface of Mars [*Malin and Edgett*, 2001] provide insight into processes occurring under current climatic conditions.

[3] Dark slope streaks were first sighted in Viking images and observed in greater detail by MGS [*Morris*, 1982; *Ferguson and Lucchitta*, 1984; *Sullivan et al.*, 2001]. Slope streaks have characteristic morphology and are typically darker than their surrounding, but occasionally the albedo contrast is reversed (Figure 1). They generally extend over distances of 100's of meters to a few kilometers longitudinally, and typically have widths of less than 200 m. Some streaks branch or fan in the downhill direction or have digitate ends. They form on slopes associated with features such as escarpments and crater walls and closely follow the local topography (Figure 1). They have hence been considered to result from gravitationally driven mass movement such as dry avalanches [*Sullivan et al.*, 2001] or wet debris [*Ferguson and Lucchitta*, 1984].

2. Data Analysis and Results

[4] In order to study the dependence of slope streak formation on environmental factors, we systematically surveyed over 23000 MOC images, of which 761 images were unambiguously identified as containing slope streaks (Figure 2), as follows. First, in a sample of 13000 MOC narrow-angle images (uniformly distributed over all latitudes) we identified 194 images with slope streaks, all in low-latitude regions. We then focused on all remaining narrow-angle images between 30°S–60°N obtained during the primary MGS mission. Streaks are grouped in three clusters, a feature best explained by comparison with the distribution of thermal inertia $I = \sqrt{k\rho c}$, where k is conductivity, ρ the density, and c the specific heat capacity (Figure 2) [*Ferguson and Lucchitta*, 1984; *Sullivan et al.*, 2001; *Rifkin and Mustard*, 2001]. The typical thermal inertia where streaks occur is 80 J m^{-2} K^{-1} $s^{-1/2}$, and 95% of slope streak images are from areas where $I < 130$ J m^{-2} K^{-1} $s^{-1/2}$. Thermal conductivity, and hence thermal inertia, strongly depends on particle size. Low thermal inertia is characteristic of dust [*Christensen*, 1986; *Jakosky and Christensen*, 1986], consistent with the interpretation of slope streaks as dust avalanches [*Sullivan et al.*, 2001].

[5] The statistics of slope streaks we have compiled allow investigation of additional correlations. We consider parameters that are averaged over regions larger than the characteristic size of slope streaks, hence these are not used to identify slope streaks individually, but rather are expected to correlate with them. While no streaks are found in areas of high thermal inertia, Figure 2 shows that some areas of low I have no streaks. Notable examples are Amazonis Planitia (16°N 202°E) and plains surrounding the Tharsis Montes (5°N 250°E), where streaks are absent. An examination of

[1]Department of Earth, Atmospheric, and Planetary Sciences, Massachusetts Institute of Technology, Cambridge, Massachusetts, USA.
[2]Division of Geological and Planetary Sciences, California Institute of Technology, Pasadena, California, USA.
[3]Now at Lamont Doherty Earth Observatory, Columbia University, Palisades, New York, USA.

0094-8276/02/2002GL015889$05.00

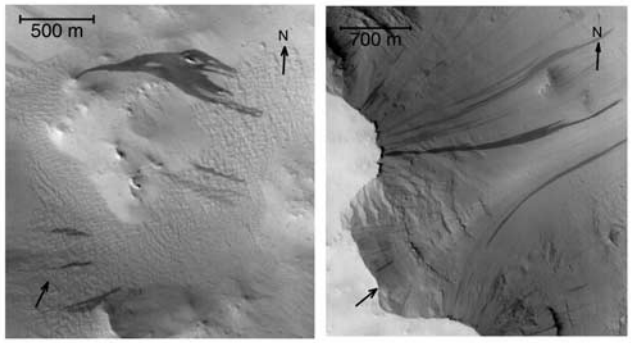

Figure 1. Examples of slope streaks in MOC narrow-angle images. Shown are subframes of images (a) M13-00834 at 143°W, 25°N and (b) M08-06185 at 35°E, 13°N. Arrows (upper right) indicate north and the direction of solar illumination (lower left). Note the strong influence of topography on the placement and orientation of streaks.

the topography reveals that those areas are particularly smooth. Figure 3 shows the root-mean-square (RMS) topographic slope (θ_r) computed from data collected by the Mars Orbiter Laser Altimeter (MOLA) [*Smith et al.*, 2001] on board MGS. The spacing of altimeter points along-track is about 300 m, comparable to the length of the streaks. The RMS of point-to-point slopes was computed in a 35 km sliding window to obtain a map of regional surface roughness [*Aharonson et al.*, 2001]. The map shows that formation of streaks is restricted to rough terrain (i.e., where steep slopes are abundant), as 95% of images with streaks occur where RMS slope values are greater than 0.9°. Smooth plains, typically associated with volcanic resurfacing, lack steep slopes and therefore slope streaks.

[6] The combined criteria of low thermal inertia ($I < 130$ J m^{-2} K^{-1} s$^{-1/2}$) and frequent steep slopes ($\theta_r > 0.9°$) account for 90% of all occurrences of slope streaks (Figure 4). While much rarer on a global average, in regions where these conditions are met, slope streaks occur in roughly one out of every five images. However, several large areas in the northern hemisphere (marked by the blue boxes on Figure 4) are sufficiently high in dust abundance and rough terrains,

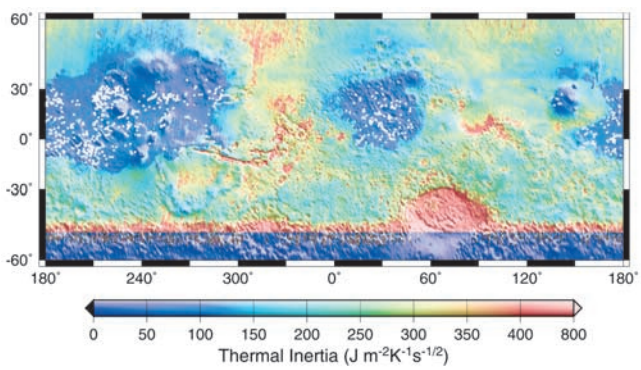

Figure 2. Thermal inertia map [*Mellon et al.*, 2000] superimposed on shaded relief. Locations of slope streaks are indicated by white dots. Streaks occur without exception in regions of low thermal inertia, thought to be covered by dust.

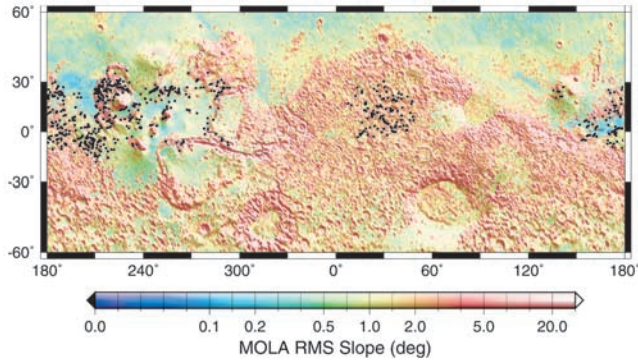

Figure 3. Map of RMS surface slope [*Aharonson et al.*, 2001] derived from MOLA elevations, superimposed on shaded relief. Slope streaks (black dots) are absent in particularly smooth terrain.

but are completely devoid of streaks. An additional control on the occurrence of slope streaks is therefore necessary.

[7] While the northern boundary between streak and streak-free images, which is zonally asymmetric, does not correspond to contrasts in mapped topography, albedo, or geologic units, it does follow a contour of surface temperature. Global coverage of temperature is available from the Thermal Emission Spectrometer (TES) on board MGS. Surface temperatures are derived from TES radiance measurements, obtained in single- and double-scan mode at a wavelength of 7μm (away from the atmospheric CO_2 absorption bands). Measurements by the Pathfinder lander [*Schofield et al.*, 1997] and model calculations [*Mellon et al.*, 2000] show that maximum temperatures occur in the early afternoon. Thus, TES-based temperatures, collected at local times between 12:50 pm and 3:00 pm provide a good estimate of the diurnal peak surface temperature. After sorting afternoon temperatures into spatial and temporal bins, the 85 percentile temperature in each bin was computed, and the yearly maximum retained. (The 75 percentile temperatures are systematically lower by about 0.5 K.) Figure 4 shows contours of peak temperature derived from data collected between February 28, 1999 and April 1, 2001, spanning more than one martian year.

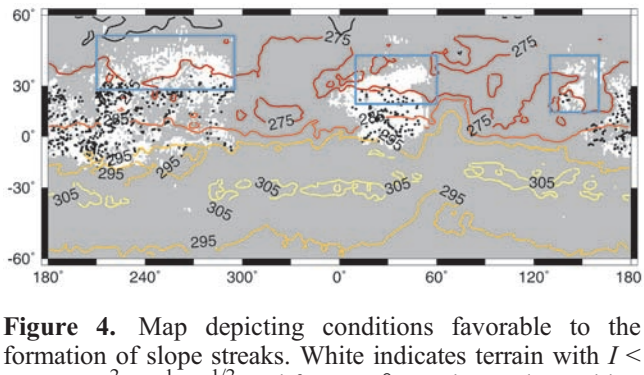

Figure 4. Map depicting conditions favorable to the formation of slope streaks. White indicates terrain with $I < 130$ J m^{-2} K^{-1} s$^{-1/2}$ and $\theta_r > 0.9°$. Regions where either condition is violated are shown in gray. Contour lines show peak temperatures, and the location of slope streaks is indicated by black dots. As seen within the areas highlighted by blue boxes, an additional control of minimum peak temperature explains the lack of slope streaks.

Table 1. Fraction of Images that Contain Slope Streaks

Condition	Percentile	Global Fraction >275K	Global Fraction <275K
$I < 115$	90%	20%	<1%
$I < 130$	95%	19%	<1%
$I < 150$	97%	18%	<1%
$I < 165$	98%	18%	<1%
$I < 130$ & $\theta_r > 0.9°$	90%	22%	<1%
$I < 150$ & $\theta_r > 0.6°$	95%	19%	<1%

The percentiles are with respect to the 761 images containing slope streaks. The global fractions are with respect to all surveyed images within the region satisfying the condition shown in the first column.

[8] The areas highlighted in Figure 4 where streaks are conspicuously missing, are separated from the areas where streaks are found by the 275 K temperature contour. It is unlikely that this temperature contour near the melting point of water coincides with the complex geographical streak boundary purely by chance. Combining the previous two criteria with a third, in which maximum temperature $T_{max} >$ 275 K, eliminates the otherwise unexplained streak-free regions in the north, and produces an excellent spatial correspondence between the combined mask and the actual locations of slope streaks (Figure 4). Table 1 demonstrates that this result is independent of the choice of threshold values.

[9] The season during which new streaks form can be constrained by repeat imaging. We have found 38 pairs of images of sites with streaks, and in addition to two previously reported image pairs with new slope streaks [*Sullivan et al.*, 2001; *Palermo, England, and Moore*, 2001 (unpublished)], we have identified five new image pairs where changes are unambiguous. Of these seven pairs, five

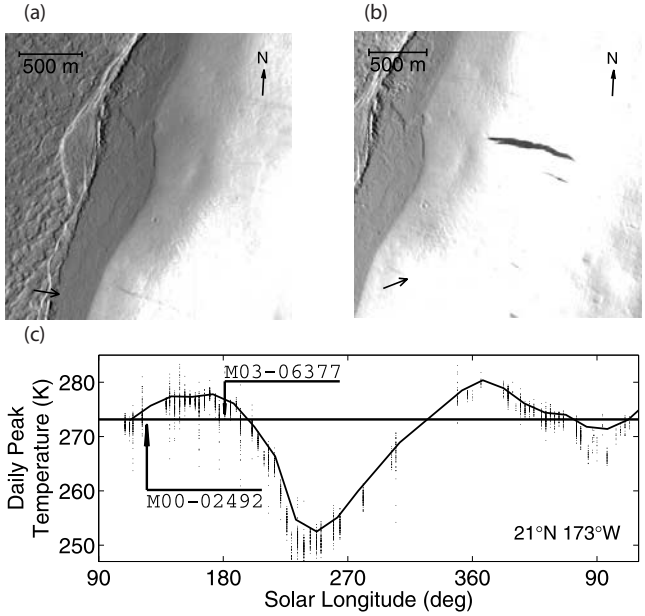

Figure 5. Daytime temperatures from TES (small dots) as a function of solar longitude L_s at a slope streak site that was imaged twice and shows newly formed streaks in the later image. To smooth the scatter in the temperature data, a line is drawn along the 85th percentile points in L_s bins of 30°. Arrows indicate the L_s at which the images were taken.

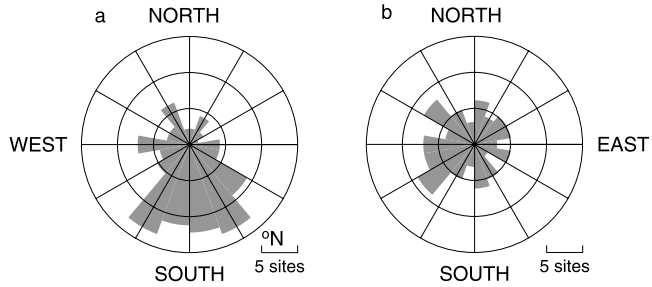

Figure 6. Histograms of streak orientations plotted as a rose diagram. Slope streaks north of 30°N (a) occur preferentially on south-facing slopes, a bias not seen in equatorial sites (b).

are less than one martian year apart and hence provide a constraint on the season during which the changes occurred. In all cases, the time interval during which new streaks formed includes periods warmer than 273 K. Figure 5 shows one example. In this small sample of image pairs, roughly 5% of streaks formed within a year.

[10] An additional line of evidence implicates temperature in the formation of streaks. Assuming that streak azimuths reflect the direction of steepest downhill gradient, a histogram of azimuths in the regions of lowest peak temperatures (latitudes north of 30°N) reveals that streaks form preferentially, though not exclusively, on equator (south) facing slopes (Figure 6a). A sample of streaks near the equator, where peak temperatures are higher and more symmetric, shows no such bias (Figure 6b).

3. The Role of Water

[11] The observed geographic (Figure 4), temporal (Figure 5), and azimuthal (Figure 6) correlations provide evidence for a connection between slope streaks and a surface temperature near the triple point of water, suggesting that the formation of streaks involves a phase transition of water. For instance, melting could provide lubrication of avalanches, or mass movements could be triggered by sublimation at the solid-gas transition. The analysis presented does not pinpoint a specific mechanism for slope streak formation, and hence we do not elaborate on any particular one, but consider the potential role of water generically. (See also *Ferris et al.* [2002].) While alternative explanations not involving water, such as patterns in atmospheric dust transport, can be envisioned, the observations are simply accounted for if water plays a role, either in triggering the mass movements or in controlling dust deposition.

[12] Below the surface, the amplitude of diurnal temperature oscillations decays exponentially, with a skin depth $\delta = (I/\rho c)\sqrt{P/\pi}$, where P is the oscillation period. For typical martian regolith (ρ = 1500 kg/m^3 and c = 630 J K^{-1} kg^{-1}) [*Mellon et al.*, 2000] in regions of low thermal inertia (I = 80), the diurnal skin depth is about 1 cm, or more if material at low thermal inertia regions is less dense [Jakosky and *Christensen*, 1986]. Temperatures above melting can occur only in the upper ~0.5 cm of the regolith. Streaks do not appear to penetrate deeply, since pre-existing surface textures are often preserved beneath the feature (e.g., Figure 1a) and no accumulated debris is visible at their termination [*Sullivan et al.*, 2001]. The small penetration depth of

melting temperatures is consistent with the interpretation that the mass flow is restricted to a thin layer.

[13] The primary atmospheric constituent is CO_2, and in a well mixed atmosphere the partial pressure of H_2O is small. However, in a static atmosphere, sublimation rates are limited by diffusion of water molecules out of a vapor layer in contact with the ice, and the partial pressure of H_2O in that layer can build up to the level of the surrounding total pressure [*Hecht*, 2002]. Many streaks occur in low-lying regions where the average pressure is above the triple point pressure of 6 mbar. However, the population of streaks extends up to 11 km elevation ($\sim$1 scale-height above the geoid) and hence to low atmospheric pressures of $\sim$2–3 mbar. The fact that the peak temperature critical for the occurrence of streaks ($\sim$275 K) is independent of pressure, suggests that sublimation in the ambient atmosphere is not the primary trigger.

[14] Dissolved salts would shift the triple point to a lower pressure (and temperature), expanding the region of stability of the liquid phase. For example, roughly 15% of NaCl would be required to lower the triple point pressure such that ice at all elevations where slope streaks occur would undergo a phase transition to liquid water during a diurnal cycle. Salinity also reduces evaporative cooling [*Ingersoll et al.*, 1970]. Alternatively, it is possible that the relevant pressure for the phase transition is not the ambient atmospheric pressure, but the pressure within isolated pore spaces or voids. Furthermore, ice is covered by a thin quasi-liquid layer well below the freezing point [*Dash et al.*, 1995], whose surface tension can increase the internal pressure within grains or at grain boundaries. Estimates for dust particle sizes range up to 40 μm [*Christensen*, 1986], which could lead to sufficient curvature effects.

[15] The possible presence of surficial H_2O at low latitudes is a surprise in light of several theoretical calculations suggesting that the residence time of any pure H_2O on the surface is short, and its long term stability unlikely [*Ingersoll*, 1970; *Farmer and Doms*, 1979]. However, H_2O can exist temporarily, over time spans that strongly depend on local conditions. For example, burial by overlying dust (perhaps catastrophically, after a dust storm) was suggested [*Farmer*, 1976; *Jakosky*, 1985] to prolong the stability of near-surface ice. Ground ice can accumulate seasonally through exchange with the atmosphere, especially in regions of low thermal inertia, and if underlain with a deeper reservoir of ice [*Paige*, 1992]. Factors such as salinity, burial, local pressure and atmospheric mixing effects, prolong ice stability [*Ingersoll*, 1970; *Farmer*, 1976; *Jakosky*, 1985; *Paige*, 1992; *Carr*, 1996; *Haberle et al.*, 2001; *Hecht*, 2002].

[16] Indeed, it is conceivable that water is only present for short times. In one such scenario dust particles stick to moist, cohesive slopes, on which they would otherwise be unstable. Dust could thus collect over temperature cycles, until at some stage (e.g., upon desiccation or critical dust-layer build-up) a collapse is triggered.

[17] The observational evidence requires neither the time over which the liquid phase exists to be long, nor the total volume of water undergoing melting or sublimation to be large. Indeed, since areas with slope streaks typically have a thermal inertia of only 80 J m^{-2} K^{-1} s$^{-1/2}$ while water ice has a high thermal conductivity and, hence, in bulk form, a high thermal inertia of $\sim$2000 J m^{-2} K^{-1} s$^{-1/2}$, large fractions of ice in the top few centimeters are unlikely. The detection of hydrogen by the Gamma Ray Spectrometer [*Boynton et al.*, 2002] on board the Mars Odyssey spacecraft lends further support to the possibility of near-surface ice.

[18] **Acknowledgments.** We thank especially M. Richardson, D. Rothman, and M. Zuber for valuable comments, and M. Mellon for supplying the thermal inertia data in digital form. The authors acknowledge the use of Mars Orbiter Camera images processed by Malin Space Science Systems. This research was funded by a DOE grant DE FG02-99ER 15004 to D. Rothman and a Mars Global Surveyor Project grant to M. Zuber. SK was supported by a William Z. Leavitt Post-Doctoral Fellowship.

References

Aharonson, O., M. T. Zuber, and D. H. Rothman, Statistics of Mars' topography from MOLA: Slopes, correlations and physical models, *J. Geophys. Res.*, *106*, 23,723–23,735, 2001.

Baker, V. R., Water and the martian landscape, *Nature*, *412*, 228, 2001.

Boynton, W. V., et al., Distribution of hydrogen in the near-surface of Mars: Evidence for subsurface ice deposits, *Science*, *297*, 81–85, 2002.

Carr, M. H., *Water on Mars*, Oxford University Press, New York, 1996.

Christensen, P. R., Regional dust deposits on Mars—physical properties, age, and history, *J. Geophys. Res.*, *91*, 3533, 1986.

Dash, J. G., H. Fu, and J. S. Wettlaufer, The premelting of ice and its environmental consequences, *Rep. Prog. Phys.*, *58*, 115–167, 1995.

Farmer, C. B., Liquid water on Mars, *Icarus*, *28*, 279–289, 1976.

Farmer, C. B., and P. E. Doms, Global and seasonal water vapor on Mars and implications for permafrost, *J. Geophys. Res.*, *84*, 2881, 1979.

Ferguson, H. M., and B. K. Lucchitta, Dark streaks on talus slopes, Mars, in *Planetary Geology and Geophysics Program Report*, pp. 188–190, 1984.

Ferris, J. C., J. M. Dohm, V. R. Baker, and T. Maddock, Dark slope streaks on Mars: Are aqueous processes involved?, *Geophys. Res. Lett.*, *29*, 10.1029/2002GL014936, 2002.

Haberle, R. M., C. P. McKay, J. Schaeffer, N. A. Cabrol, E. A. Grin, A. P. Zent, and R. Quinn, On the possibility of liquid water on present-day Mars, *J. Geophys. Res.*, *106*, 23,317–23,331, 2001.

Hecht, M. H., Metastability of liquid water on Mars, *Icarus*, *156*, 373, 2002.

Ingersoll, A. P., Mars: Occurrence of liquid water, *Science*, *168*, 972–973, 1970.

Jakosky, B. M., The seasonal cycle of water on Mars, *Space Sci. Rev.*, *41*, 131–200, 1985.

Jakosky, B. M., and P. R. Christensen, Global duricrust on Mars: Analysis of remote-sensing data, *J. Geophys. Res.*, *91*, 3547, 1986.

Malin, M. C., and K. S. Edgett, Evidence for recent groundwater seepage and surface runoff on Mars, *Science*, *288*, 2330, 2000.

Malin, M. C., and K. S. Edgett, Mars Global Surveyor Mars Orbiter Camera: Interplanetary cruise through primary mission, *J. Geophys. Res.*, *106*, 23,429, 2001.

Mellon, M. T., B. M. Jakosky, H. H. Kieffer, and P. R. Christensen, High-resolution thermal inertia mapping from the Mars Global Surveyor Thermal Emission Spectrometer, *Icarus*, *148*, 437, 2000.

Morris, E., Aureole deposits of the Martian volcano Olympus Mons, *J. Geophys. Res.*, *87*, 1164, 1982.

Paige, D. A., The thermal stability of near-surface ground ice on Mars, *Nature*, *356*, 43–45, 1992.

Rifkin, M. K., and J. F. Mustard, Global distribution of unique surface processes imaged by the Mars Orbital Camera, in *Lunar and Planetary Science Conf.*, vol. XXXII, Houston, Texas, abstract 1968, 2001.

Schofield, J. T., et al., The Mars Pathfinder atmospheric structure investigation meteorology (ASI/MET) experiment, *Science*, *278*, 1752, 1997.

Smith, D. E., et al., Mars Orbiter Laser Altimeter: Experiment summary after the first year of global mapping of Mars, *J. Geophys. Res.*, *106*, 23,689–23,722, 2001.

Sullivan, R., P. Thomas, J. Veverka, M. Malin, and K. S. Edgett, Mass movement slope streaks imaged by the Mars Orbiter Camera, *J. Geophys. Res.*, *106*, 23,607, 2001.

O. Aharonson and N. Schorghofer, MC 150-21, California Insitute of Technology, Pasadena, CA 91125, USA. (norbert@segovia.mit.edu)

S. Khatiwala, Oceanography 201, Lamont Doherty Earth Observatory, Columbia University, Palisades, NY 10964, USA.